Proceedings of IMECE '01
2001 International Mechanical Engineering Congress and Exhibition
November 11-16, 2001, New York, New York, USA

THERMAL MODELING OF UNLOOPED AND LOOPED PULSATINHG HEAT PIPES

M. B. Shafii, Amir Faghri, Yuwen Zhang[1]

Department of Mechanical Engineering
University of Connecticut
Storrs, CT 06269-3139
Email: faghri@engr.uconn.edu

ABSTRACT

Analytical models for both unlooped and looped Pulsating Heat Pipes (PHPs) with multiple liquid slugs and vapor plugs are presented in this study. The governing equations are solved using an explicit finite difference scheme to predict the behavior of vapor plugs and liquid slugs. The results show that the effect of gravity on the performance of top heat mode unlooped PHP is insignificant. The effects of diameter, charge ratio, and heating wall temperature on the performance of looped and unlooped PHPs are also investigated. The results also show that heat transfer in both looped and unlooped PHPs is due mainly to the exchange of sensible heat.

NOMENCLATURE

A	undisturbed radius of inner surface of condensate film, m
A	tube cross sectional area, m^2
B	number of bends
C_l	friction coefficient
c_p	specific heat (constant pressure), J/kg K
c_v	specific heat (constant volume), J/kg K
d	diameter, m
g	gravitational acceleration, m^2/s
h	enthalpy, J/kg
h_c	heat transfer coefficient at the cooling section, W/m^2K
h_{fg}	latent heat, J/kg
h_h	evaporative heat transfer coefficient, W/m^2K
L	length, m
L_h	length of heating section, m
L_c	length of cooling section, m
m	mass, kg
$\dot{m}$	mass flow rate, kg/s
N	total number of vapor plugs
n	number of parallel tubes
N_p	total number of plugs
P	pressure, Pa
Pr	Prandtl number
R	gas constant, J/kgK
Re	Reynolds number
t	time, s
u	internal energy, J/Kg
T	temperature, K
V_v	volume of vapor, m^3
v_l	velocity of liquid plug, m/s
X	distance, m

Greek Symbols

α	charge ratio
α_l	thermal diffusivity of liquid, m^2/s
λ	wavelength, m
μ	dynamic viscosity, kg/ms
ρ	density, kg/m^3
τ	shear stress, N/m^2

[1] Presently at Department of Mechanical Engineering, New Mexico State University, Las Cruces, NM 88003.

θ_{max} maximum contact angle
θ_{min} minimum contact angle

Subscripts
in inlet
li *i*th liquid plug
le left end
out outlet
re right end
vi *i*th vapor plug

INTRODUCTION

Downsizing of personal computers and advancing performance of processors has called for the development of micro and miniature heat pipes [1,2] to transport heat from chips to heat sinks. The Oscillating or Pulsating Heat Pipe (OPH or PHP) is a very promising heat transfer device [3]. In addition to its excellent heat transfer performance, it has a simple structure: in contrast with conventional heat pipes, there is no wick structure to return the condensed working fluid back to the evaporator section. The PHP is made from a long, continuous capillary tube bent into many turns. The diameter of the PHP must be sufficiently small so that vapor plugs can be formed by capillary action. The PHP is operated within 0.1-5 mm inner diameter range. If the diameter is too large, the liquid and vapor phases will tend to stratify. The PHP can operate successfully for all operation modes, including both horizontal and vertical. Due to the pulsation of the working fluid in the axial direction of the tube, heat is transported from the evaporator section to the condenser section. The heat input, which is the driving force, increases the pressure of the vapor plug in the evaporator section. In turn, this pressure increase will push the neighboring vapor plugs and liquid slugs toward the condenser, which is at a lower pressure. However, due to the continuous heating of bubbles formed by nucleate boiling, there will not be steady-state vapor pressure equilibrium for an operating PHP. There are two types of PHPs: the looped PHP, which has two open ends, connected to one another, and the unlooped PHP, which has two unconnected ends.

Active oscillations of working fluid were observed at charging ratios of 40~60% for a vertical looped PHP. With this charge ratio range, the circulation velocity is at maximum value which results in best heat transfer performance. It has been reported that the looped heat pipe is better than the unlooped heat pipe for heat transfer performance [4]. In an unlooped PHP, the working fluid is unable to circulate and the heat is transferred by driving force due to the oscillation. Gi *et al.* [5] investigated an 'O' shaped oscillating heat pipe as it applied to the cooling of a CPU. Their results showed that the temperature of a CPU chip with a power less than 40W rises to 90 ^{0}C, which is the maximum temperature for the safe use of notebook computers. They were able to make a very small thermal resistance heat transfer system between a CPU with the power of 40W and cooling fins. To predict the oscillatory flow characteristics, Miyazaki and Arikawa [6] proposed a theoretical model, which was strongly supported by experimental results. The visualization test showed that the oscillatory flow formed waves that traveled among the turns of PHPs. Their theoretical model could be used to estimate the pressure and displacement of oscillatory flow. Kiseev and Zolkin [7] experimentally investigated the effects of acceleration and vibration on the performance of the unlooped PHP. Acetone was used as the working fluid and the filling charge ratio was 60%. Their results indicated that the PHP operates successfully by various acceleration effects. There was an increase in evaporator temperature, about 30% by increase of the acceleration from -6g to +12g.

Dobson and Harms [8] presented simple mathematical models in which the behavior of PHPs was simulated. The mathematical model was applied to the open-ended PHP. They showed that the oscillating behavior would be different for different initial values. Wong *et al.* [9] proposed a theoretical model of PHPs based on a Lagrangian approach in which the flow was modeled under adiabatic conditions for the entire PHP. A sudden pressure pulse was applied to simulate local heat input into a vapor plug. They were able to show the pressure and velocity variations with time for the vapor plugs.

In the present study, a very detailed theoretical model will be developed to accurately simulate the behavior of liquid slugs and vapor plugs in both unlooped and looped PHPs. Heat transfer due to the phase change is also considered.

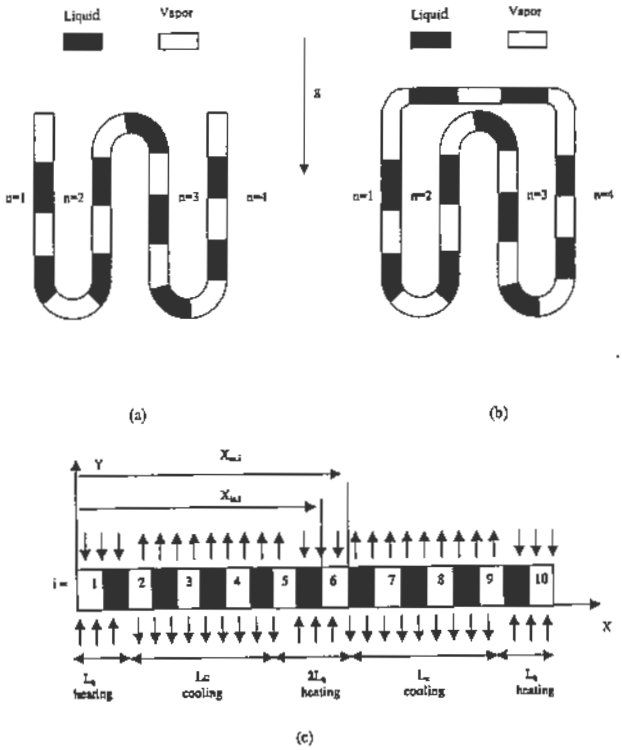

Fig. 1 Pulsating heat pipes

Table 1 Summary of experimental works on pulsating heat pipe data

Investigators	Type and heat (mode of PHP)	Cross section of tubes	Number of parallel tubes	Length of each tube (cm)	Charging Ratio (%)	Working fluid	Length of Liquid slug (cm)	Length of vapor plug (cm)	D (mm)	Initial length of liquid slug required by stability (mm)	Initial liquid slug length by eq. (4) (mm)	Comments
Gi et al. [13]	Looped (Vertical bottom)	Circular	20	50	30-70	R-142b	NA	NA	2	4.4	2.66	The effect of charging ratio, operating temperature and inclination angle
Gi et al. [13]	Unlooped (Vertical bottom)	Circular	20	50	30-70	R142b	NA	NA	2	4.4	2.66	The effect of charging ratio and inclination angle
Lee et al. [4]	Looped (Vertical bottom)	Rectangular	8	22	20-80	Ethanol	NA	NA	1.5	3.33	7.48	Nucleate boiling observed, Most active oscillation at charging ratio of 40-60% and the inclination angle of 90°
Maczawa et al. [12]	Unlooped (Horizontal) (Vertical top) (Vertical bottom)	Circular	41	60	40-50	Water R-142b	NA	NA	2	4.4	14.88 2.66	Top mode operated very well. R-142b was better working fluid. Non-periodic dynamics System was governed
Miyazaki and Arikawa [6]	Looped (Vertical top)	Rectangular	50	27.3	42	R142b	21.84	32.76	NA	-	-	Analytical model was proposed for circulation of wave velocity
Miyazaki and Akachi [13]	Looped (Vertical bottom) (Horizontal)	Circular	31	20	26-70	R142b	NA	NA	1	2.22	5.32	Circulation was observed. An analytical model was proposed.
Nishiho [14]	Looped (Vertical bottom)	Circular	8	39.6	20-100	Water Ethanol R-142b	NA	NA	1.8 2.4 5	Water Ethanol R 142b 4 4 4 5.33 5..33 5.33 11.1 11.1 11.1	Water Ethanol R 142b 16.53 16.53 2.96 12.4 4.67 2.22 5.95 2.24 1.06	The total temperature difference between hot and cold water in heating and cooling section varied (30-60°C)

THEORITICAL MODEL

Initial Plug Distribution

When a capillary tube is partially filled, the working fluid will break into liquid slugs and vapor plugs (see Fig. 1(a)). Hosoda *et al.* [10] conducted a numerical analysis for bubble geometry in a tube and determined the maximum inner diameter that can hold a vapor plug.

$$D_{max} = 1.84\sqrt{\frac{\sigma}{g(\rho_l - \rho_v)}} \tag{1}$$

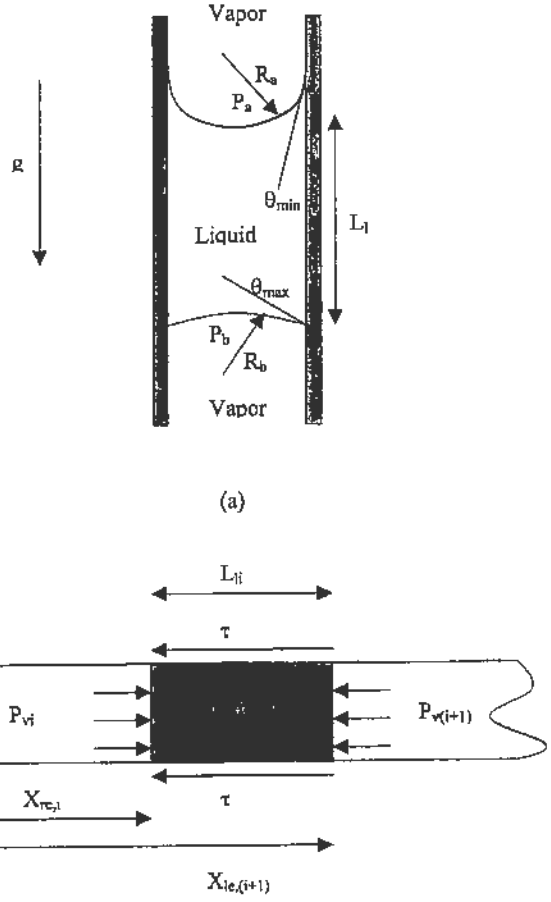

Fig. 2 (a) Control volume of *a* liquid slug in a vertical tube; (b) Control volume of i^{th} liquid plug

D_{max} is about 2.5mm for saturated water at 300K and thus a tube of 1.5mm is chosen in the present study. A simple momentum equation can be solved in order to predict the length of liquid slugs. When a slug of liquid is formed in a vertical tube, gravity naturally tends to pull the liquid downward. However, as downward motion begins, the contact angles at top and bottom of the liquid plug must be receding and advancing, respectively. Fig. 2(a) shows a control volume of a liquid slug bounded with two vapor plugs in a vertical tube. Force balance requires that

$$P_{va}\pi R^2 - P_{vb}\pi R^2 + \rho_l g L_l \pi R^2 + 2\pi R_b \sigma - 2\pi R_a \sigma = 0 \tag{2}$$

$$P_{vb} - P_{va} = \rho_v g L_l \tag{3}$$

Combining eq. (3) into (2) results in

$$L_l = \frac{2\sigma}{R(\rho_l - \rho_v)g}\left(\cos\theta_{min} - \cos\theta_{max}\right) \tag{4}$$

Assuming that θ_{min} and θ_{max} have minimum and maximum values, one can find the length of the liquid slugs that can be supported against gravity. It should be noted that eq. (4) is valid only when the pressure difference between the two vapor plugs has such a relation as eq. (3). However, when the unlooped heat pipe is partially filled, it is less likely to display the relationship between pressures of vapor plugs expressed as eq. (3). In this case instability theory of condensate film and capillary blocking in small diameter tube can be used to predict the initial length of liquid slugs. Teng *et al.* [11] investigated instability of the condensate film in small diameter tubes using an integro-differential approach. They mentioned that liquid bridging caused by the breakup of condensate film originates from capillary instability. This breakup of condensate film causes the formation of liquid slugs. The film instability results from surface tension and the length of the disturbance waves, which can be approximated as a function of the radius of the undisturbed inner condensate film. The most-unstable wavelength can be obtained from [11]

$$\lambda_m = \sqrt{8}\pi a \tag{5}$$

where *a* is the undisturbed radius of the condensate film inner surface and is assumed to be half the size of the tube radius. The length of liquid slugs can be predicted from eq. (5) by assuming the most-unstable wavelength to be the length of the liquid slugs. Table 1 is the summary of the experimental works on the pulsating heat pipes. The predicted lengths of the liquid slugs obtained from eq. (4) and eq. (5) are also included in this table.

Governing Equations

The oscillatory phenomenon in PHPs can be predicted by solving mass, momentum and energy equations for each liquid slug and vapor plug. The schematics of unlooped and looped PHPs are shown in Fig.1(a) and (b). The bends are not considered in the present study and the PHP is assumed to be a straight tube (see Fig. 1(c)). The locations and the number of heating and cooling sections represent the number of bends or turns in actual PHPs. There are three heating sections and two cooling sections on the PHP. The inner wall temperature at the

heating and cooling sections of the PHP are T_h and T_c, respectively. A control volume of a liquid slug bounded with two vapor plugs is shown in Fig. 2(b).

To solve the problem analytically, the following assumptions are made:

1. Evaporative and condensation heat transfer coefficients are assumed to be constants.
2. The liquid is incompressible and the vapor plugs are assumed to behave as an ideal gas in the heating sections.
3. The pressure losses at the bends are not considered. This assumption is valid for the PHPs do not have many turns. When the number of turns is larger, the pressure loss at the turns may not be negligible.

The continuity equation for ith liquid slug can be found from following equation

$$\frac{d\,m_{li}}{dt} = \dot{m}_{in,li} - \dot{m}_{out,li} = \frac{1}{2}\left(\frac{dm_{vi}}{dt} + \frac{dm_{v(i+1)}}{dt}\right) \tag{6}$$

This means that the change in mass of liquid slug is equal to the average changes in mass of its adjacent vapor plugs. The momentum equation for ith liquid slug, assuming the PHP operates vertically, is

$$\frac{dm_{li}v_{li}}{dt} = (P_{vi} - P_{v(i+1)})A - \pi dL_{li}\tau - (-1)^n m_{li}g \tag{7}$$

where n indicates the tube number. Since it is assumed that the PHP is a straight tube, gravity has different signs at different locations. In this model, there are four parallel tubes, which are labeled from one to four (Fig. 1). The heating section is located at the top of the PHP. Gravity vector is in positive direction when a liquid slug is in the first or third tubes; therefore, the gravity term in eq. (7) is positive. In the second or fourth tubes the gravity vector is in the opposite direction and the gravity force term in eq. (7) is negative. τ is the shear stress acting between ith liquid slug and the tube and can be determined from

$$\tau = \frac{1}{2}C_{li}\rho_l v_{li}^{\,2} \tag{8}$$

where the friction coefficient can be determined by

$$C_{li} = \begin{cases} \dfrac{16}{\mathrm{Re}} & \mathrm{Re} \le 1180 \\ 0.078\,\mathrm{Re}^{-0.2} & \mathrm{Re} > 1180 \end{cases} \tag{9}$$

The continuity equation for the ith vapor plug is

$$\frac{dm_{vi}}{dt} = \dot{m}_{in,vi} - \dot{m}_{out,vi} \tag{10}$$

where $\dot{m}_{in,vi}$ is the rate of mass transferred into the vapor plug due to the evaporation and $\dot{m}_{out,vi}$ is the rate of mass transferred from the vapor plug due to the condensation for ith vapor plug and can be calculated by the following equations:

$$\begin{aligned} \dot{m}_{in,vi} &= (h_h + h_{vsen})\pi dL_{hi}(T_{vi} - T_h)/h_{fg} \\ \dot{m}_{out,vi} &= (h_c + h_{vsen})\pi dL_{ci}(T_c - T_{vi})/h_{fg} \end{aligned} \tag{11}$$

It is assumed that the evaporative heat transfer coefficient, h_h, is constant as long as one of the ends of the vapor plug is in the heating section. When the two ends are out of the heating section, the liquid film in the evaporator dries out and the evaporative heat transfer is zero. The sensible heat transfer coefficient, h_{vsen}, is negligible in comparison with the evaporative heat transfer coefficient. The energy equation of a vapor plug is

$$\frac{dm_{vi}u_{vi}}{dt} = \dot{m}_{in,vi}\,h_{in,vi} - \dot{m}_{out,vi}\,h_{out,vi} - P_{vi}\frac{dV_{vi}}{dt} \tag{12}$$

Letting $u = c_v T$ and $h = c_p T$, equation (12) may be rewritten as

$$m_{vi}c_v\frac{dT_{vi}}{dt} = (\dot{m}_{in,vi} - \dot{m}_{out,vi})RT_{vi} - P_{vi}A\frac{dX_{vi}}{dt} \tag{13}$$

The pressure of the ith vapor plug, P_{vi} is calculated using the ideal gas law

$$P_{vi}V_{vi} = m_{vi}RT_{vi} \tag{14}$$

It is important to note that the pressure, calculated from eq. (14), cannot exceed the saturation pressure corresponding to the temperature calculated from eq. (13). When the vapor pressure, calculated by eq. (14), is lower than the saturation pressure, the vapor plug is superheated and the ideal gas law is valid. On the other hand, if the vapor pressure, calculated by eq. (14), is higher than saturation pressure, the ideal gas law is no longer valid and the pressure is set to the saturation pressure calculated by

$$P_{vi} = P_{sat}(T_{vi}) \tag{15}$$

Heat Transfer

Heat transfer in a PHP is defined as total heat transferred from heating sections to the cooling sections. Part of heat transfer is due to evaporation and condensation of working fluid. Another part is due to heat transfer between tube wall and liquid slugs in the form of single-phase heat transfer. Evaporative and condensation heat transfer for each vapor plug can be calculated by

$$Q_{in,vi} = \dot{m}_{in,vi}\, h_{fg}$$

$$Q_{out,vi} = \dot{m}_{out,vi}\, h_{fg} \tag{16}$$

The single-phase heat transfer between the tube wall and liquid slugs is obtained by solving the energy equation for a liquid slug

$$\frac{1}{\alpha_l}\frac{dT_{li}}{dt} = \frac{d^2T_{li}}{dx^2} - \frac{h_{lsen}\pi D}{k_l A}(T_{li} - T_w) \tag{17}$$

with the following boundary conditions

$$\begin{aligned} T_{li} &= T_{vi} && x = x_{re,i} \\ T_{li} &= T_{v(i+1)} && x = x_{le,(i+1)} \end{aligned} \tag{18}$$

Since the Reynolds number of the liquid slug varies in a wide range that covers laminar, transition, and turbulent flow, the heat transfer coefficient h_{lsen} of the liquid slug varies from time to time. For laminar regime, (Re < 2200), the problem is considered as thermally developing Hagen-Poiseuille flow and the Nusselt number is

$$Nu = \frac{1}{4L_l^*}\ln\left(\frac{1}{\theta^*_m}\right) \tag{19}$$

where

$$\theta^*_m = 8\sum_{n=0}^{\infty}\frac{G_n}{\lambda^2_n}\exp(-2\lambda^2_n L_l^*) \tag{20}$$

The eigenvalues, λ_n, and the constants, G_n, can be found in Ref. [15]. The dimensionless L_l^* is defined as

$$L_l^* = \frac{L_{li}/D}{\mathrm{Re}_D\,\mathrm{Pr}} \tag{21}$$

In the transition and turbulent regions, the following empirical equations are used

$$Nu = 0.012(|\mathrm{Re}|^{0.87} - 280)\,\mathrm{Pr}^{0.4}\left(\frac{\mathrm{Pr}_m}{\mathrm{Pr}_w}\right)^{0.11}\left[1+\left(\frac{D}{L_{li}}\right)^{\frac{2}{3}}\right]$$

$$2200 < |\mathrm{Re}| < 10000 \tag{22}$$

$$Nu = 0.0236|\mathrm{Re}|^{0.8}\,\mathrm{Pr}^{0.43}\left(\frac{\mathrm{Pr}_m}{\mathrm{Pr}_w}\right)^{0.25} \qquad |\mathrm{Re}| > 10000 \tag{23}$$

The heat transferred into and out of the liquid slug is

$$Q_{in,li} = \int_{X_{re,i}}^{X_{le,(i+1)}} \pi D h_x (T_{li,x} - T_w)dx \quad T_{li} \ge T_w \tag{24a}$$

$$Q_{out,li} = \int_{X_{re,i}}^{X_{le,(i+1)}} \pi D h_x (T_w - T_{li,x})dx \quad T_{li} \le T_w \tag{24b}$$

where $T_{li,x}$ represents the temperature of the i^{th} liquid plug at location x. The total heat transferred into and out of the PHP can be calculated by

$$Q_{total,in} = \sum_{i=1}^{N} Q_{in,iv} + \sum_{i=1}^{N-1} Q_{in,li} \tag{25a}$$

$$Q_{total,out} = \sum_{i=1}^{N} Q_{out,iv} + \sum_{i=1}^{N-1} Q_{out,li} \tag{25b}$$

NUMERICAL PROCEDURE

The new values at time t + dt can be found explicitly from the old values at time t by using the following equations:

$$m_{vi}^{new} = m_{vi} + (\dot{m}_{in,vi} - \dot{m}_{out,vi})\Delta t \tag{26}$$

$$T_{vi}^{new} = T_{vi} + \frac{(\dot{m}_{in,vi} - \dot{m}_{out,vi})RT_{vi}\Delta t - P_{vi}A\Delta X_{vi}}{m_{vi}c_v} \tag{27}$$

$$P_{vi}^{new} = \frac{m_{vi}RT_{vi}}{V_{vi}} \tag{28}$$

$$m_{li}^{new} = m_{li} + \frac{1}{2}\left[(\dot{m}_{in,vi} - \dot{m}_{out,vi}) + (\dot{m}_{in,v(i+1)} - \dot{m}_{out,v(i+1)})\right]\Delta t \tag{29}$$

$$m_{li}^{new} v_{li}^{new} = m_{li}v_{li} + \left[(P_{vi} - P_{v(i+1)})A - \pi d L_{li}\tau + m_{li}g\right]\Delta t \tag{30}$$

The determinations of the locations of liquid slugs and vapor plugs are different for unlooped and looped PHPs.

Unlooped PHP

The position of each vapor plug is known by the location of its ends one can write

$$\begin{cases} X_{re,i}^{new} = X_{re,i} + v_{li}\Delta t \\ X_{le,i}^{new} = X_{le,i} + v_{l(i-1)}\Delta t \end{cases} \tag{31}$$

$$\begin{cases} X_{re,N} = L \\ X_{le,1} = 0 \end{cases} \tag{32}$$

where N is the number of vapor plugs. X is measured from the origin showed in Fig.1(b).

$$\begin{cases} \Delta X_{re,i}^{new} = X_{re,i}^{new} - X_{re,i} \\ \Delta X_{le,i}^{new} = X_{le,i}^{new} - X_{le,i} \end{cases} \quad (33)$$

$$\begin{aligned} \Delta X_{re,N}^{new} &= 0 \\ \Delta X_{le,1}^{new} &= 0 \end{aligned} \quad (34)$$

$$\Delta X_{vi}^{new} = \Delta X_{re,i}^{new} - \Delta X_{le,i}^{new} \quad (35)$$

where ΔX_{vi}^{new} is the change in length of the ith vapor plug. $\Delta X_{re,i}$ and ΔX_{zi-1} are the changes in location of the ends of the ith vapor plug.

Looped PHP

The looped PHP is similar to the unlooped PHP except its two ends are connected to each other (Fig 1.(b)). Governing equations used for unlooped PHPs are valid for looped PHPs, except that the first and last vapor plugs (shown in Fig. 1(b)) are basically one vapor plug, and both of them have the same values of pressure and temperature. The position of the two ends of the vapor plugs is found from the following equations:

$$\begin{cases} X_{re,i}^{new} = X_{re,i} + v_{re,i}\Delta t \\ X_{le,i}^{new} = X_{le,i} + v_{le,(i-1)}\Delta t \end{cases} \quad (36)$$

$$\begin{cases} X_{re,i}^{new} = X_{re,i}^{new} - L & X_{re,i}^{new} > L \\ X_{le,i}^{new} = X_{le,i}^{new} - L & X_{le,i}^{new} > L \end{cases} \quad (37)$$

$$\begin{cases} X_{re,i}^{new} = X_{re,i}^{new} + L & X_{re,i}^{new} < 0 \\ X_{le,i}^{new} = X_{le,i}^{new} + L & X_{le,i}^{new} < 0 \end{cases} \quad (38)$$

$$\Delta X_{vi}^{new} = \Delta X_{re,i}^{new} - \Delta X_{le,i}^{new} \quad (39)$$

The last two equations guarantee that the position of the two ends of the vapor plug remains between 0 and L. Time step independence of the numerical solution for both unlooped and looped PHP was verified by systematically varying the time step. It was found that varying the time step from 5×10^{-6} s to 10^{-8}s results in less than 0.2% variation in the locations of the liquid slugs. Therefore, the time step used in the numerical solution is 5×10^{-6} s.

To find the sensible heat transferred by the liquid slugs, eq. (17) is solved using an implicit scheme [16]. A nonuniform grid was chosen to solve the energy equation of liquid slugs. The total number of grids chosen is 360, with 140 belonging to each end (2 cm) and 80 grids in the middle of each liquid slug. Doubling the number of grids does not change the solution results. Since decreasing the time step to 10^{-4}s results in 0.2% variation in temperature distribution along the liquid slugs, the time step used in the numerical solution is 10^{-3}s.

RESULTS AND DISSCUSSION

Evolution of Flow Pattern

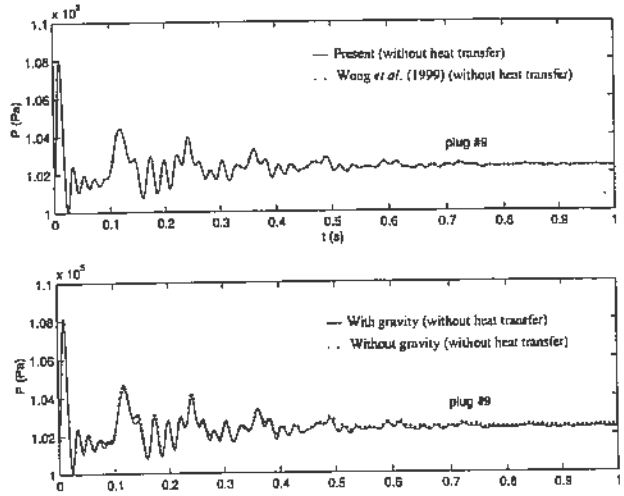

Fig. 3 Comparison of the pressure variation with time; (a) without gravity; (b) with gravity; (c) comparison with a previous model

Table 2. Initial values of PHP

Initial pressure of vapor plugs	$T_{vi} = 35\ ^0C$
Percentage filled	$\alpha = 61.4\%$
Initial temperature of vapor plugs	$T_{vi} = 35\ ^0C$
Total length	L = 1.14 m
Total number of plugs	$N_p = 5$
Number of bends	B = 3
Length of each vapor plug	$L_{v1}=L_{v2}=0.11$ m
Cooling section wall temperature	$T_c = 20\ ^0C$
Heating section wall temperature	$T_h = 120\ ^0C$
Heat transfer coefficient at heating wall	$h_h = 150$ W/m^2 ^{0}C
Heat transfer coefficient at cooling wall	$h_c = 100$ W/m^2 ^{0}C
Diameter	d = 0.0015 m
Length of heating section	$L_h = 0.1$m
Length of cooling section	$L_c = 0.37$m

The verification of the numerical method was performed by simulating the propagation of pressure waves inside a PHP [9]. The capillary heat pipe is modeled under adiabatic conditions. A sudden pressure pulse is applied to a plug at one end of the PHP to study the pressure variation with time. A total of 20 liquid slugs and vapor plugs existing in the pipe. The length of all vapor and liquid plugs was assumed to be

identical. An initial pressure of 1.1 times higher than the rest is applied to the 10th vapor plug. The comparison between the present result and that of Ref. [9] for the 9th plug is presented in Fig. 3(a). It can be seen that the agreement between the present numerical results and the results of Wong *et al.* [9] is excellent for the case with no heat transfer. Fig. 3(b) shows the effect of gravity on the pressure variation. It is seen that the effect of gravity on pressure variation is not significant, and therefore it can be neglected in the numerical model.

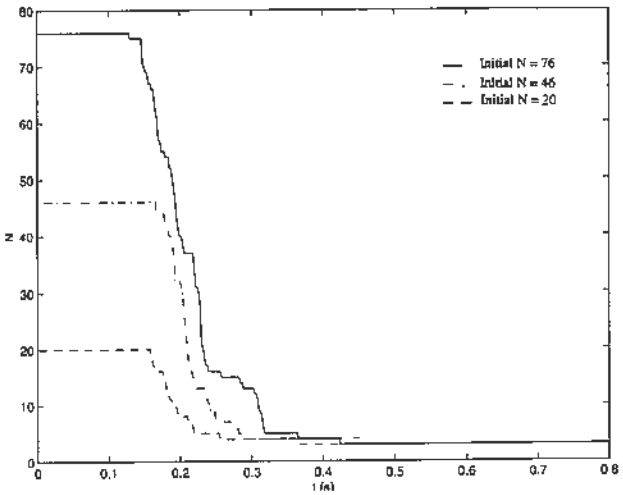

Fig. 4 Variation of the total number of vapor plugs

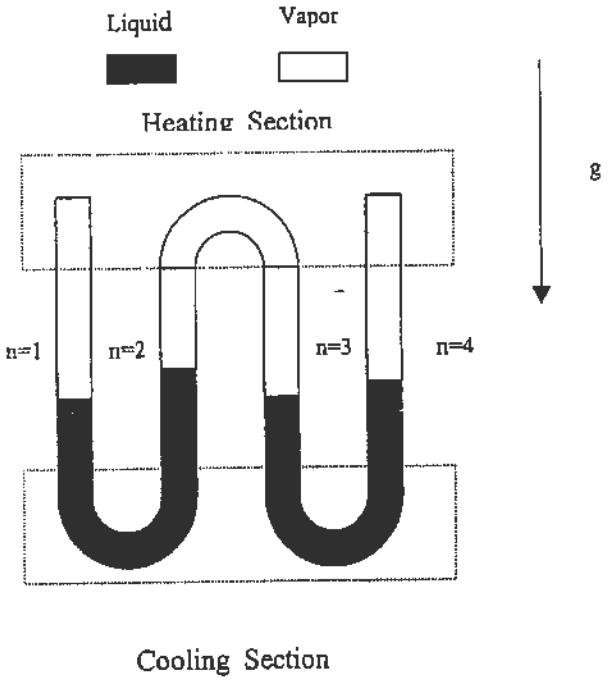

Fig. 5 Unlooped PHP including three vapor plugs

When the heating sections are heated and cooling sections are cooled, the pressure of vapor plugs located in the cooling sections is lower than that of vapor plugs in the heating sections, since the temperature is lower. This pressure difference causes the liquid slugs to move toward cooling sections and consequently the volume of vapor plugs in cooling sections decreases until the adjacent liquid slugs merge to one another and the vapor plugs diminish. Fig. 4 shows the variation of the total number of vapor plugs with time when unlooped PHP is exposed to heating and cooling conditions. The parameters used in the numerical simulation are listed in Table 2 except that the total number of vapor plugs varies. The number of vapor plugs eventually reduces to three, which is equal to the number of heating sections. This means that vapor plugs exist only in heating sections, no matter how many vapor plugs are initially in the PHP (see Fig. 5). It can also be observed that when the total initial number of vapor plugs is high, the evolutionary time is high.

Unlooped PHP

The parameters used are listed in Table 2. An initial pressure of 1.2 times higher than the rest is applied to the first vapor plug. The lengths of liquid slugs are equal and can be found based on the charge ratio of the system. Therefore, the parametric study of PHP in the following section will be performed for three vapor plugs in the heating sections. Figure 6 shows the variations of pressure, temperature and positions of the two ends of the first vapor plug with respect to time. Initially, both the temperature and pressure drop to certain values, since the right end of the first vapor plug is located in the cooling section and condensation takes place. When the pressure is low enough, the adjacent liquid slug starts moving back toward the heating section, and as it moves back, the temperature of the vapor plug increases due to the compression. However, condensation is still taking place. When the right end moves into the heating section, evaporation takes place. The pressure and temperature of vapor plug keep increasing until the pressure in the vapor plug is high enough to push the adjacent liquid slug toward the cooling section. This phenomenon repeats itself and periodic oscillation occurs after almost 10 s. The temperature of the first vapor plug is maximum, or equal to the heating wall temperature, when it is completely compressed in the heating section. At this point its pressure is also maximum at 6×10^4 Pa. Since the pressure is lower than saturated pressure, the vapor plug is super heated. Fig. 6(c) shows the position of the two ends of the first vapor plug. Since the first vapor plug is located at the end of the PHP, the left end is always located at $x = 0$ m. The right end oscillates between $x = 0.08$ m and $x = 0.14$ m.

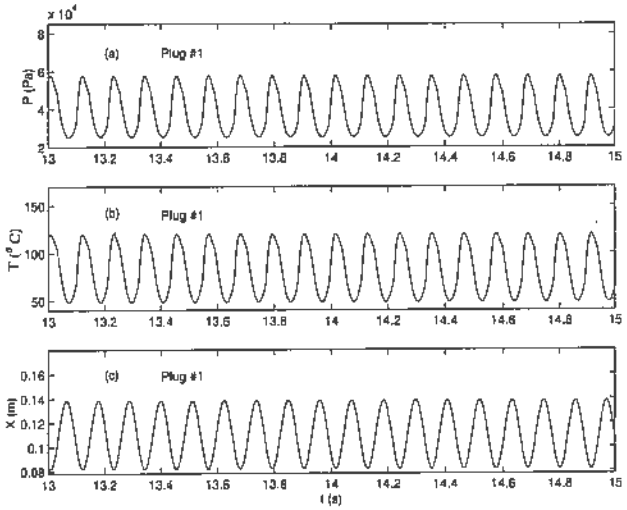

Fig. 6 Variation of pressure, temperature and the end positions of the first plug with time (d = 1.5mm)

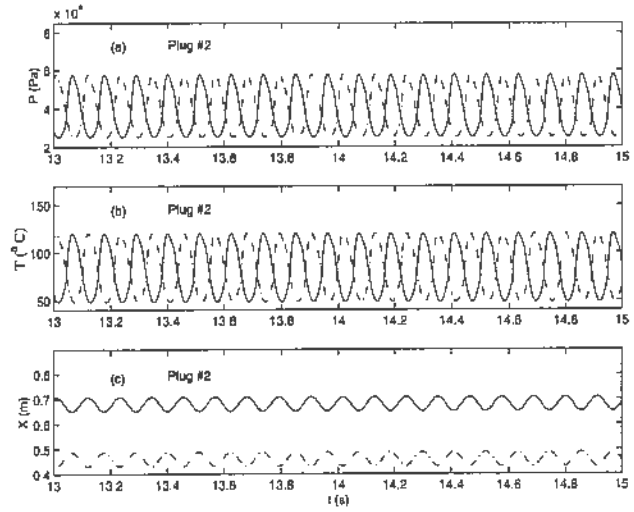

Fig. 7 Variation of pressure, temperature and theend positions of the second plug with time (d = 1.5mm)

Figure 7 shows the variations of pressure, temperature and positions of the two ends of the second vapor plug. Since the two ends are free to move into heating and cooling sections, the frequencies of the pressure and temperature oscillation are equal to that of the first vapor plug and the phase difference is 180^0. Fig 7(c) shows the position of two ends of this vapor plug. The solid and dashed lines represent the location of the right and left ends. The distance between these two lines indicates the length of the vapor plug. The two ends always move in opposite directions and they move into either the cooling or heating sections. Figure 8 represents pressure, temperature and position of the two ends of the third vapor plug variations with time. Since the system is symmetric, the oscillating trends of pressure temperature and position of the ends are the same as those of the first vapor plug and there is no phase difference between the oscillations.

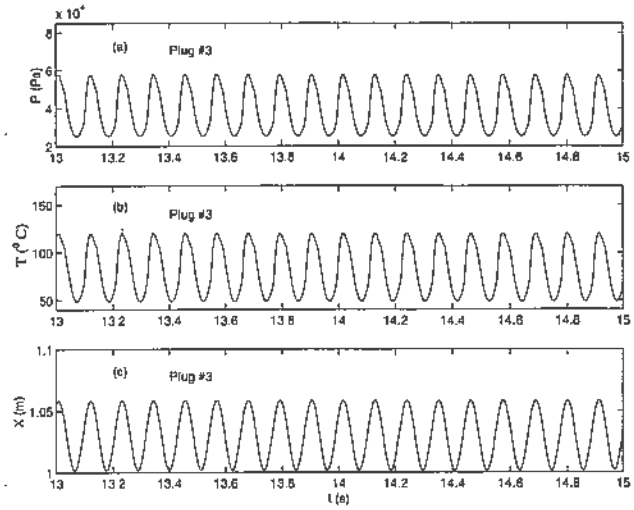

Fig. 8 Variation of pressure, temperature and the end positions of the third plug with time (d = 1.5mm)

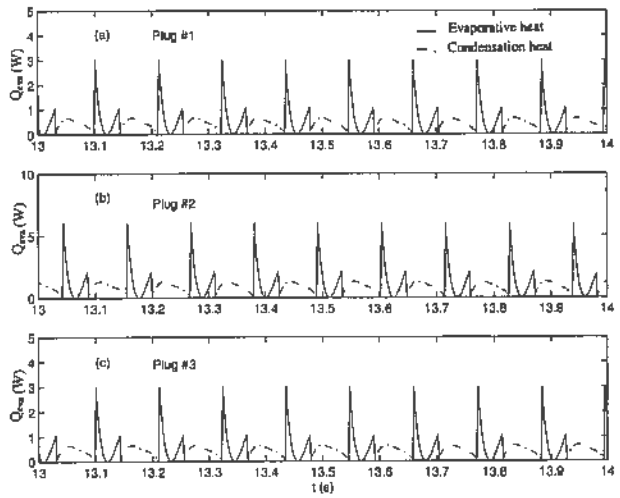

Fig. 9 The evaporative and condensation heat transfer rate

The rate of evaporative and condensation heat transfer of each individual vapor plug, when periodic oscillation is obtained, is shown in Fig. 9. It can be seen from Fig. 9(a) that when the right end of the first vapor plug moves into the heating section, the evaporative heat transfer suddenly jumps to its maximum value. Then it starts decreasing to its minimum value as the right end continues moving inside the heating section and compresses the first vapor plug. Meanwhile, the vapor plug temperature increases due to evaporation and compression. As the vapor expands, its temperature drops and heat transfer increases until the right end moves into the cooling section where condensation occurs. Fig. 9(b) and 9(c) show the same behavinr for the second and third plugs.

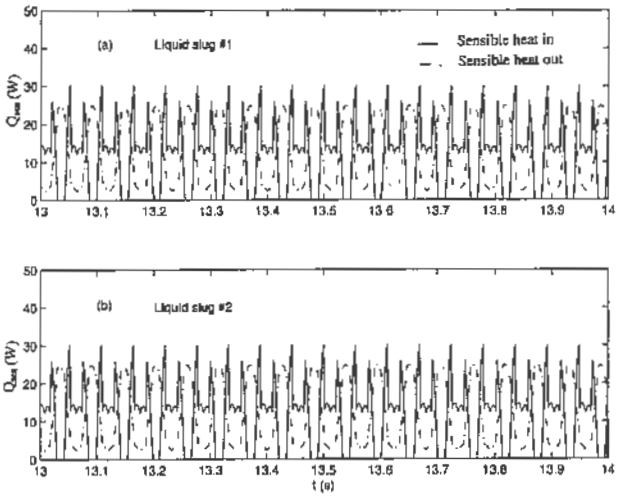

Fig. 10 Sensible heat transferred in and out of liquid slugs

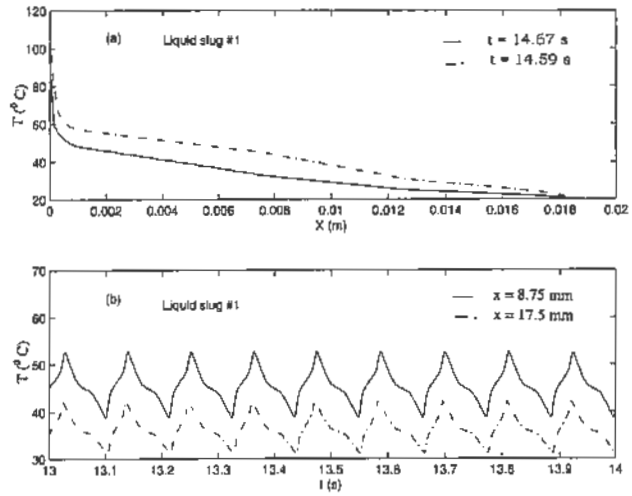

Fig. 11 Temperature of the first liquid slug; (a) distribution along the left end of the first liquid slug; (b) variation with time

The variation of the sensible heat transferred into and out of the liquid slugs is shown in Fig. 10. The solid line represents heat transferred into the liquid slugs from heating sections and the dashed line represents the heat rejected from the liquid slugs into the cooling systems. When the liquid slugs are completely in the cooling sections, there is no sensible heat transferred into the slugs and the heat rejected from the slugs is at its maximum. The sudden changes in the sensible heat are due to the change from laminar flow to transition flow. The maximum Reynolds number for liquid slugs is Re = 4200. Figure 11(a) shows temperature distribution of the left end of the first liquid slug. The distance is measured from the tip of the left end of the first liquid slug. Only 2.5 cm of the left end moves into the heating section and contributes in transferring heat. Since the middle part always remains in the cooling section, its temperature is always at the cooling wall temperature (20^0C). Figure 11(b) shows the temperature variation of two selected points on the left end of the first liquid slug. One is 4.37mm (solid line) and the other one is 8.75 mm (dashed line) away from the left end. The one closer to the left end has a higher temperature because it remains longer in the heating section. The total heat transferred into the PHP for this case is 24.88W. The total sensible heat transferred is 23.84W and this means that 95.84% heat transferred into the system is due to the sensible heat. To investigate the effect of diameter on performance of the PHP, the diameter of the tube is increased to 3 mm. The other parameters and initial values are not changed. Figure 12 (a) shows the pressure variation with time for the first vapor plug. It can be observed that the frequency of oscillation is higher than that of the small diameter tube. From Fig. 12 (b) and 12 (c) one can conclude that the average temperature of the first vapor plug is the same as that of the first vapor plug in the small diameter tube by the time the right end moves into the heating section (see at t = 14.95 s). However, since the heating area is greater than that of the small diameter tube, the evaporative heat is higher for all vapor plugs (Fig. 13). The total heat transferred into the PHP for this case is 80.17 W. Results indicate that the contribution of the sensible heat is 97.12% of the total heat.

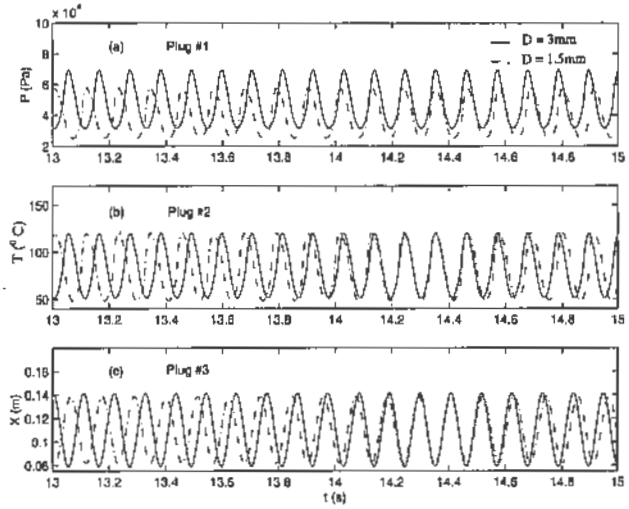

Fig. 12 Effect of the diameter of PHP on the performance of the first vapor plug

Figure 14 shows the effect of heating wall temperature on pressure, temperature and end positions of the first plug. The parameters and thermal properties are similar to what is given in Table 2, except that the wall temperature is reduced to 90^0C. Decreasing the wall temperature results in the decreased magnitude of pressure and the location of the right end and it also slightly decreases the frequency of oscillation. It can be seen from Fig. 14(b) that the average temperature of the first vapor plug decreases when the wall temperature decreases and the temperature difference between the wall and vapor plug is lower. This results in lower evaporative heat transfer shown in Fig. 15. This figure indicates that the heat transferred into the vapor plugs decreased with decreasing the temperature difference between heating and cooling section. The total heat

transferred into the PHP for this case is 8.35 W. Results indicate that the contribution of the sensible heat is 92.54% of the total heat transfered. From calculated results, it can be concluded that a 25% reduction in the temperature difference between heating and cooling wall sections results in almost 90% reduction in total heat transferred into the PHP.

Table 3 Effect of parameters on the performance of the PHPs

Type of PHP	T (c	Charge ratio %	D (mm)	Evaporative heat (W)	Sensible heat (W)	Total heat transfer (W)
Unlooped	120	61.4	1.5	1.035	23.84	24.88
	90	61.4	1.5	0.62	7.73	8.35
	120	61.4	3	2.3	77.87	80.17
	120	89.47	1.5	0	0	0
Looped	120	61.4	1.5	1.2	23.83	24.99
	90	61.4	1.5	6	7.73	8.36
	120	61.4	3	2.24	77.13	79.37
	120	89.47	1.5	0	0	0

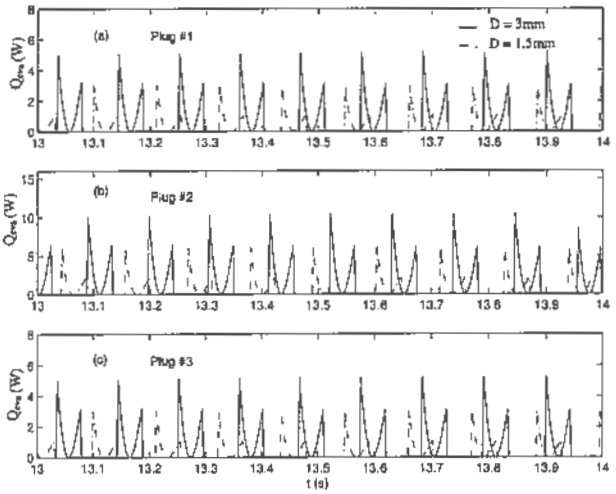

Fig. 13 Effect of PHP diameter on the total evaporative heat transfer rate

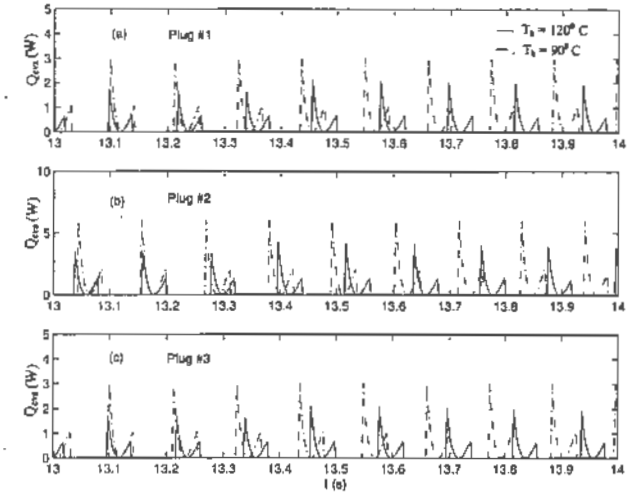

Fig. 15 Effect of the heating wall temperature on the total evaporative heat transfer rate

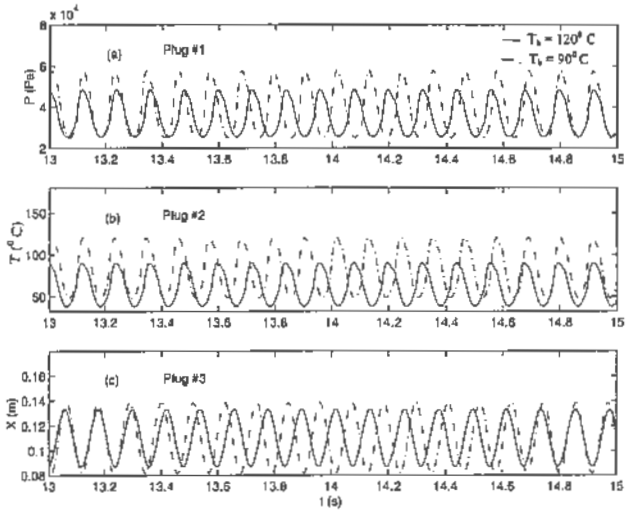

Fig. 14 Effect of the heating wall temperature on the performance of the first plug

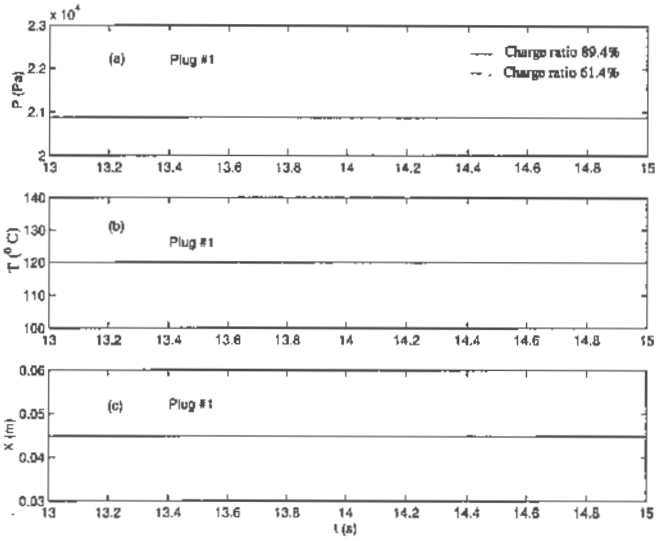

Fig. 16 Effect of the charge ratio on the performance of the first plug

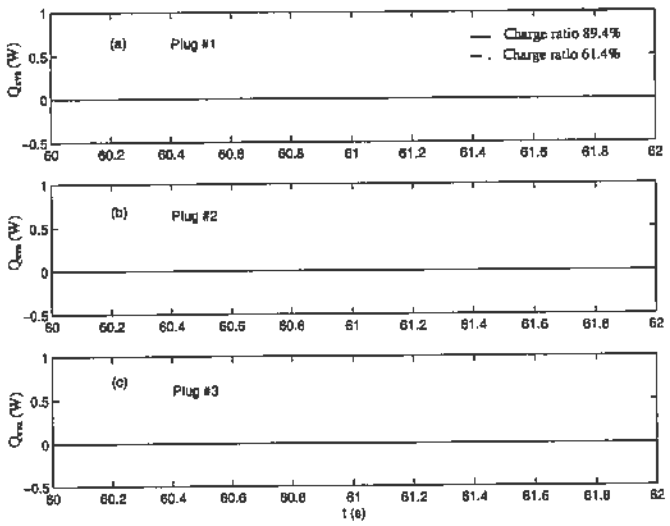

Fig. 17 Effect of the charge ratio on the total evaporative heat transfer rate

The effect of charging ratio on the performance of the PHP is shown in Fig. 16. The tube diameter is 1.5 mm. The length of all liquid slugs is 0.51 m. Therefore, the first and third vapor plugs would have the length of 0.03 m and the second one would be twice as long as the other two. This yields a charge ratio of 89.4% in the PHP. Figure 16 indicates that oscillation cannot be obtained when the charging ratio is high. When the charging ratio is high in the PHP, the liquid slugs are long, and a higher-pressure difference is needed to move more massive liquid slugs. Since this pressure difference cannot be obtained, the temperature rises to the wall temperature. As a result, no heat will be transferred into the plugs (Fig. 17) and the PHP will not perform properly. This prediction is consistent with experimental results presented by Gi *et al.* [17]. Their results showed that heat transport rate decreased with increasing charge ratio for unlooped PHP. The effect of different parameters, as discussed above, on the heat transfer performance of the unlooped PHP is listed in Table 3.

Looped PHP

Miyazaki and Arikawa [6] performed visualization experiments on looped PHPs and observed that liquid slugs and vapor plugs were almost separated into two parts in the individual turns. Liquid was observed at the cooling side, forming a U-shaped column, while vapor was observed at the heating side. This means that, similar to the unlooped PHP, vapor plugs exist only in heating sections. The behavior of liquid slugs and vapor plugs in looped PHPs is also investigated. The parameters specified in Table 2 are used except that the total number of plugs is N = 4. Also, the length of the first and second vapor plugs would be equal due to the fact that the first and the last vapor plugs are connected to make one plug. Figure 18 (a) shows the variations of the pressure of the first and second vapor plugs with time. Figure 18 (b) shows the variation of the temperatures. Since the system is symmetric, the phase difference between oscillation of the first and last plugs is 180^0. Figure 18 (c) represents the oscillation of the two ends of the second vapor plug. Figure 19(a) shows the sensible heat transferred into the liquid slugs. Both the first and the second slugs have the same phase and amplitude, since they move at the same velocity in opposite directions. Figure 19(b) shows the evaporative heat transferred into the vapor plugs. The amplitudes of the oscillation of the two plugs are equal, but there is a phase difference of 180^0. The total heat transferred into the PHP for this case is 24.95 W. Results indicate that the contribution of the sensible heat is 95.50% of the total heat. The effects of changes in diameter, heating wall temperature and charge ratio on the heat transfer performance of looped PHPs are also investigated, and the summarized results are shown in Table 3. Increasing the diameter and heating wall temperature increases the total heat transfer similar to that of the unlooped PHP. It can also be observed that increasing the charge ratio to 90% will stop the performance of looped PHPs. Calculated results show no circulation in the system, which is consistent with the visualization of Lee *et al.* [4] and Miyazaki and Arikawa [6].

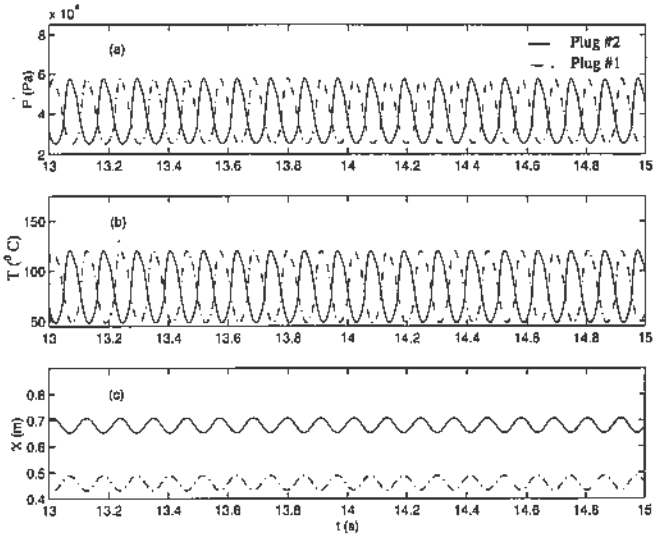

Fig. 18 Variation of pressures, temperatures and the end positions the first and second plugs with time for looped PHP (d = 1.5mm)

CONCLUSIONS

Thermal modeling of both unlooped and looped PHPs with multiple vapor plugs and liquid slugs is proposed, and the behaviors of liquid and vapor plugs in the PHP are investigated. The following conclusions were obtained:

1. The results show that gravity does not have significant effect on the performance of unlnoped PHPs with top heat mode.
2. The total number of vapor plugs reduced to the total number of heating sections, no matter how many vapor plugs were initially in the system.

3. For both looped and unlooped PHPs, periodic oscillation is obtained under specified parameters.
4. Heat transfer in both looped and unlooped PHPs is due mainly to the exchange of sensible heat. The role of evaporation and condensation on the performance of the PHPs is mainly on the oscillation of liquid slugs.
5. By increasing the diameter of the PHP (both looped and unlooped), the total average heat transfer increases.
6. Decreasing the temperature of the heating wall sections significantly decreases the total average heat transfer. This means that the temperature difference between heating and cooling walls is significant in the total amount of heat transferred.
7. The results also showed that both looped and unlooped PHPs did not operate for higher charging ratios.

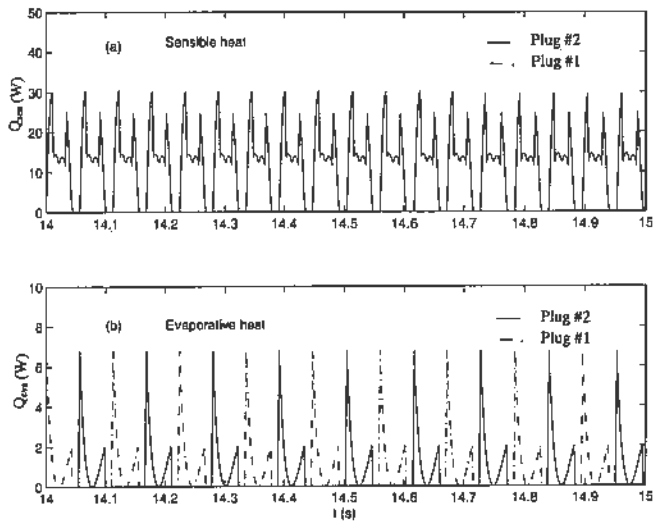

Fig. 19 Variation of heat transfer rate with time for looped PHP; (a) sensible heat; (b) evaporative and condensation heat

ACKNOWLEDGEMENT

Funding for this work was provided by NASA grant NAG3-1870 and NSF grant CTS 9706706.

REFERENCES

1. Faghri, A., 1995, *Heat Pipe Science and Technology*, Taylor & Francis, Washington, DC.

2. Faghri, A., 1999, Recent Advances and Challenges in Micro/Miniature Heat Pipes, *Proceedings of 11th International Heat Pipe Conference*, Tokyo, Japan

3. Akachi, H., 1994, *Looped Capillary Heat Pipe*, Japanese Patent, No. Hei6-97147.

4. Lee, W.H., Jung, H.S., Kim, J.H., and Kim J.S., 1999, Flow Visualization of Oscillating Capillary Tube Heat Pipe, *Proceedings of 11th International Heat Pipe Conference*, Tokyo, Japan, pp. 131-136

5. Gi, K., and Maezawa, S., Kojima, Y., and Yamazaki, N. 1999 a, CPU Cooling of Notebook PC by Oscillating Heat Pipe, *Proceedings of 11th International Heat Pipe Conference*, Tokyo, Japan, pp. 166-169.

6. Miyazaki, Y, and Arikawa, M., 1999, Oscillatory Flow in The Oscillating Heat Pipe, *Proceedings of 11th International Heat Pipe Conference*, pp. 143-148, Tokyo, Japan.

7. Kiseev, V.M., and Zolkin, K.A., 1999, The Influence of Acceleration on The Performance of Oscillating Heat Pipe, *Proceedings of 11th International Heat Pipe Conference*, Tokyo, Japan, pp. 154-158.

8. Dobson, R.T., and Harms, T.M. 1999, Lumped Parameter Analysis of Closed and Open Oscillatory Heat Pipes, *Proceedings of 11th International Heat Pipe Conference*, Tokyo, Japan, pp. 137-142.

9. Wong, T.N., Tong, B.Y., Lim, S.M., and Ooi, K.T., 1999, Theoretical Modeling of Pulsating Heat Pipe, *Proceedings of 11th International Heat Pipe Conference*, Tokyo, Japan, pp. 159-163.

10. Hosoda, M., Nishio, S., and Shirakashi, R., 1999, Meandering Closed-Loop Heat-Transport tube (Propagation Phenomena of Vapor Plug), *Proceedings of the 5th ASME/JSME joint Thermal Engineering Conference*, March 15-19, San Diego, CA.

11. Teng, H., Cheng, P., and Zhao, T.S., 1999, Instability of Condensate Film and Capillary Blocking in Small-Diameter-Thermosyphon Condensers, *International Journal of Heat and Mass Transfer*, 42, 3071-3083.

12. Maezawa, S., Nakajima, R., Gi, K, and Akachi, H., 1996, Experimental Study on Chaotic Behavor of Thermohydraulic Oscillation in Oscillating Thermosyphon, *Proceedings of 5th International Heat Pipe Symposium*, Melbourne, Australia, pp. 131-137

13. Miyazaki, Y., and Akachi, H., 1996, Heat Transfer Characteristics of Looped Capillary Heat Pipe, *Proceedings of 5th International Heat Pipe Symposium*, Melbourne, Australia, pp. 378-383.

14. Nishio, S., 1999, Oscillatory-Flow Heat-Transport Device (Forced Oscillatory Flow Type and Bubble Driven Type), *Proceedings of 11th International Heat Pipe Conference*, Tokyo, Japan, pp. 39-50.

15. Bejan, B., 1995, *Convection Heat Transfer*, John Wiley & Sons, Inc, 2nd edition, New York.

16. Patankar, S.V., 1980, *Numerical Heat Transfer and Fluid Flow*, McGraw-Hill, New York.

17. Gi, K., Sato, F., and Maezawa, S., 1999 b, Flow Visualization Experiment on Oscillating Heat Pipe, *Proceedings of 11th International Heat Pipe Conference*, Tokyo, Japan, pp. 149-153.